A Novel Performance Evaluation of Power Quality Features Using Hybrid FACTS Device with Induction Motor

Bugatha Ram Vara Prasad , Thatithuri Satish Babu , Kezhiyur Alfoni Jose , Majji Satish

Assistant Professor Department of Electrical & Electronics Engineering, Lendi Institute of Engineering and Technology, Jonnada, Vizianagaram (Dist), A.P, India.

ramvaraprasad205@gmail.com , satishthatithuri@gmail.com , alfonijose.kezhiyur@lendi.org , majji.satish486@gmail.com

Abstract –*in this paper research work is directed to study of some controllers for design, modelling, simulation and hybrid facts device by implementation of induction motor (IM) drive system to identify suitable controller for high performance. Initially dynamic modelling and simulation of a feedback linearization scheme for high performance IM drive is carried out. Shunt Hybrid Active Filter is constituted by Active Filter connected in shunt and shunt connected three phase single tuned LC filter for 5th harmonic frequency with rectifier load. The simulation results are listed in comparison of different control strategies and induction motor characteristicsfor the verification of results.*

Index Terms—Harmonic Suppression, Hybrid Power filter, Modelling, Shunt Hybrid Power filter AndThyristor-Controlled Reactor (SHPF-TCR Compensator).

I. INTRODUCTION

In recent years, Power engineers are increasingly concerned over the quality of theelectrical power. In modern industries, load equipment uses electronic controllers which aresensitive to poor voltage quality and will shut down if the supply voltage is depressed and maymal-operate in other ways if harmonic Distortion of the supply voltage is excessive. Most of thismodern load equipment uses electronic switching devices which can contribute to poor networkvoltage quality [1].

The competition in electrical energy supply has created greater commercialawareness of the issues of power quality while equipment is readily available to measure thequality of the voltage waveform and so quantify the problem.Along with advance technology, the organization of the worldwide economy has evolvedtowards globalization and the profit margins of many activities tend to decrease [2, 3]. The increasedsensitivity of the vast majority of processes like (industrial, services and even residential) to PQproblems turn the availability of electric power with quality a crucial factor for competitiveness inevery sector. The continuous process industry and the information technology services are mostcritical area. Due to disturbance, a huge amount of financial losses may happen, with theconsequent loss of productivity and competitiveness.Many efforts have been taken by utilities to full fill consumer requirement, some consumersrequire a higher level of power quality than the level provided by modern electric networks [5-8].

Thisimplies that some measures must be taken so that higher levels of Power Quality can be obtained.The FACTS devices and Custom power devices are introduced to electrical system toimprove the power quality of the electrical power. DVR, DSTATCOM, ACTIVE FILTERs,UPQC etc. are some of the devices used to improve the power quality of the voltage and current.With the help of these devices we are capable to reduce the problems related to power quality.Although all devices can improve the power quality but in this the focus is onUPQC.UPQC is a power electronic device consisting of both DVR and D-STATCOM, former isconnected in series and latter is connected in parallel to protect the sensitive load from alldisturbances [9,10].

Hence, the proposed combination of SHPF and TCR compensates for unwanted reactive power and harmonic currents. In addition, it reduces significantly the volt-ampere rating of the APF part. The control method of the combined compensator is presented. A control technique is proposed to improve the dynamic response and decrease the steady-state error of the TCR. It consists of a PI controller and a lookup table to extract the required firing angle to compensate a reactive power consumed by the load. A nonlinear control of SHPF is developed for current tracking and voltage regulation purposes. It is based on a decoupled control strategy, which considers that the controlled system may be divided into an inner fast loop and an outer slow one [11-14].

II. SYSTEM CONFIGURATION OF SHPF-TCR COMPENSATOR

Fig. 1 shows the topology of the proposed combined SHPF and TCR. The SHPF consists of a small-rating APF connected in series with a fifth-tuned LC passive filter. The APF consists of a three-phase full-bridge voltage-source pulse width modulation (PWM) inverter with an input boost inductor (L_{pf}, R_{pf}) and a dc bus capacitor (C_{dc}). The APF sustains very low fundamental voltages and currents of the power grid, and thus, its rated capacity is greatly reduced. Because of these merits, the presented combined topology is very appropriate in compensating reactive power and eliminating harmonic currents in power system. The tuned passive filter in parallel with TCR forms a shunt

passive filter (SPF). This latter is mainly for fifth harmonic compensation and PF correction. The small-rating APF is used to filter harmonics generated by the load and the TCR by enhancing the compensation characteristics of the SPF aside from eliminating the risk of resonance between the grid and the SPF. The TCR goal is to obtain a regulation of reactive power. The set of the load is a combination of a three phase diode rectifier and a three-phase star-connected resistive inductive linear load.

III. MODELING AND CONTROL STRATEGY

A. Modeling of SHPF

The system equations are first elaborated in 123 reference frame. Using Kirchhoff's voltage law, one can write

$$v_{s1} = L_{PF}\frac{di_{c1}}{dt} + R_{PF}i_{c1} + v_{CPF1} + v_{1M} + v_{MN}$$

$$v_{s2} = L_{PF}\frac{di_{c2}}{dt} + R_{PF}i_{c2} + v_{CPF2} + v_{2M} + v_{MN}$$

$$v_{s3} = L_{PF}\frac{di_{c3}}{dt} + R_{PF}i_{c3} + v_{CPF3} + v_{3M} + v_{MN}$$

$$v_{CPF1} = L_T\frac{di_{c1}}{dt} - C_{PF}L_T\frac{d^2v_{CPF1}}{dt^2}$$

$$v_{CPF2} = L_T\frac{di_{c2}}{dt} - C_{PF}L_T\frac{d^2v_{CPF2}}{dt^2}$$

$$v_{CPF3} = L_T\frac{di_{c3}}{dt} - C_{PF}L_T\frac{d^2v_{CPF3}}{dt^2}$$

$$\frac{dv_{dc}}{dt} = \frac{1}{C_{dc}}i_{dc}. \tag{1}$$

The switching function ck of the kth leg of the converter (for $k = 1, 2, 3$) is defined as

$$c_k = \begin{cases} 1, & \text{if } S_k \text{ is On and } S_k' \text{ is Off} \\ 0, & \text{if } S_k \text{ is Off and } S_k' \text{ is On.} \end{cases} \tag{2}$$

A switching state function d_{nk} is defined as

$$d_{nk} = \left(c_k - \frac{1}{3}\sum_{m=1}^{3}c_m\right)_n \tag{3}$$

Moreover, the absence of the zero sequence in the ac currents and voltages and in the $[d_{nk}]$ functions leads to the following transformed model in the three-phase coordinates:

$$L_{PF}\frac{di_{c1}}{dt} = -R_{PF}i_{c1} - d_{n1}v_{dc} - v_{CPF1} + v_{s1}$$

$$L_{PF}\frac{di_{c2}}{dt} = -R_{PF}i_{c2} - d_{n2}v_{dc} - v_{CPF2} + v_{s2}$$

$$L_{PF}\frac{di_{c3}}{dt} = -R_{PF}i_{c3} - d_{n3}v_{dc} - v_{CPF3} + v_{s3}$$

$$C_{dc}\frac{dv_{dc}}{dt} + \frac{v_{dc}}{R_{dc}} = d_{n1}i_{c1} + d_{n2}i_{c2} + d_{n3}i_{c3}. \tag{4}$$
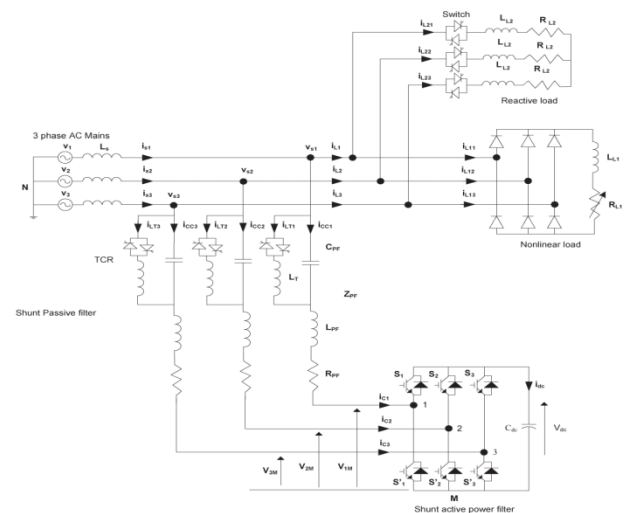

Fig.1. Basic circuit of the proposed SHPF-TCR compensator.

The system of (4) is transformed into the synchronous orthogonal frame using the following general transformation matrix:

$$C_{dq}^{123} = \sqrt{\frac{2}{3}}\begin{bmatrix} \cos\theta & \cos(\theta - 2\pi/3) & \cos(\theta - 4\pi/3) \\ -\sin\theta & -\sin(\theta - 2\pi/3) & -\sin(\theta - 4\pi/3) \end{bmatrix} \tag{5}$$

where $\theta = \omega t$ and the following equalities hold:

$$C_{123}^{dq} = (C_{dq}^{123})^{-1} = (C_{dq}^{123})^T$$

Then, by applying dq transformation, the state space model of the system in the synchronous reference frame

This model is nonlinear because of the existence of multiplication terms between the state variables $\{i_d, i_q, V_{dc}\}$ and the switching state function $\{d_{nd}, d_{nq}\}$. However, the model is time invariant during a given switching state.

Furthermore, the principle of operation of the SHPF requires that the three state variables have to be controlled independently. The interaction between the inner current loop and the outer dc bus voltage loop can be avoided by adequately separating their respective dynamics.

B. Harmonic Current Control

A fast inner current loop, and a slow outer dc voltage loop, is adopted. The first two equations in the model can be written as shown in the Appendix by (27). Note

that the first and the second time derivative TCR capacitor voltages have no significant negative impact on the performance of the proposed control technique because their coefficients are too low. Consequently, they can practically be ignored. Define the equivalent inputs by (28) as given in the Appendix.
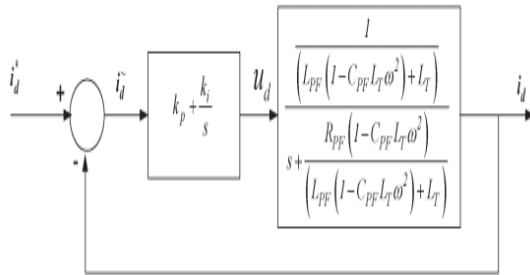

Fig.2.Inner control loop of the current i_d.

Thus, with this transformation, the decoupled dynamics of the current tracking is obtained. The currents i_d and i_q can be controlled independently. Furthermore, by using proportional integral compensation, a fast dynamic response and zero steady-state errors can be achieved. The expressions of the tracking controllers are

$$u_d = \left(L_{PF}(1 - C_{PF}L_T\omega^2) + L_T\right)\frac{di_d}{dt} + R_{PF}(1 - C_{PF}L_T\omega^2)i_d$$

$$= k_p\tilde{i}_d + k_i\int \tilde{i}_d dt$$

$$u_q = \left(L_{PF}(1 - C_{PF}L_T\omega^2) + L_T\right)\frac{di_q}{dt} + R_{PF}(1 - C_{PF}L_T\omega^2)i_q$$

$$= k_p\tilde{i}_q + k_i\int \tilde{i}_q dt$$

The transfer function of the proportional–integral controllers is given as

$$G_{i1}(s) = \frac{U_d(s)}{\tilde{i}_d(s)} = k_{p1} + \frac{k_{i1}}{s}$$

$$G_{i2}(s) = \frac{U_q(s)}{\tilde{i}_q(s)} = k_{p2} + \frac{k_{i2}}{s} \quad (7)$$

The inner control loop of the current id is shown in Fig.3.2. The closed-loop transfer functions of the current loops are

$$\frac{I_d(s)}{I_d^*(s)} = \frac{k_{p1}}{A} \frac{\left(s + \frac{k_{i1}}{k_{p1}}\right)}{s^2 + \left(\frac{B + k_{p1}}{A}\right)s + k_{i1}}$$

$$\frac{I_q(s)}{I_q^*(s)} = \frac{k_{p2}}{A} \frac{\left(s + \frac{k_{i2}}{k_{p2}}\right)}{s^2 + \left(\frac{B + k_{p2}}{A}\right)s + k_{i2}} \quad (8)$$

The closed-loop transfer functions of the current loops have the following form:

$$\frac{I_d(s)}{I_d^*(s)} = 2\zeta\omega_{ni} \frac{s + \frac{\omega_{ni}}{2\zeta}}{s^2 + 2\zeta\omega_{ni}s + \omega_{ni}^2}$$

where ω_{ni} is the outer loop natural angular frequency and ζ is the damping factor. For the optimal value of the damping factor $\zeta = \sqrt{2}/2$, the theoretical overshoot is 20.79%. The followingdesign relations can be derived:

$$k_{p1} = k_{p2} = 2\zeta\omega_{ni}\left(L_{PF}(1 - C_{PF}L_T\omega^2) + L_T\right) - R_{PF}(1 - C_{PF}L_T\omega^2)$$

$$k_{i1} = k_{i2} = \left(L_{PF}(1 - C_{PF}L_T\omega^2) + L_T\right)\omega_{ni}^2$$

The control law is given in the Appendix by (29) and (30). Note that the inputs q_{nd} and q_{nq} consist of a nonlinearity cancellation part and a linear decoupling compensation part.

C. DC Bus Voltage Regulation

In order to maintain the dc bus voltage level at a desired value, acting on i_q can compensate the losses through the hybrid power filter components. The output of the controller is added to the q-component current reference i_q as shown in Fig. 4. The third equation in the model (6) is rewritten

$$C_{dc}\frac{dv_{dc}}{dt} + \frac{v_{dc}}{R_{dc}} = d_{nq}i_q \quad (10)$$

The three-phase filter currents are given by

$$\begin{bmatrix} i_{c1} \\ i_{c2} \\ i_{c3} \end{bmatrix} = \sqrt{\frac{2}{3}}i_q \begin{bmatrix} -\sin\theta \\ -\sin\left(\theta - \frac{2\pi}{3}\right) \\ -\sin\left(\theta - \frac{2\pi}{3}\right) \end{bmatrix} \quad (11)$$

The fundamental filter RMS current I_c is

$$I_c = \frac{i_q}{\sqrt{3}}. \quad (12)$$

The q-axis active filter voltage v_{Mq} is expressed as

$$v_{Mq} = q_{nq}v_{dc} = -Z_{PF1}i_{q1}^* \quad (13)$$

where Z_{PF1} is the impedance of the passive filter at 60 Hz and i_{q1}^* is a dc component.

An equivalent input u_{dc} is defined as

International Journal of Research
Available at https://edupediapublications.org/journals

e-ISSN: 2348-6848
p-ISSN: 2348-795X
Volume 04 Issue-17
December 2017

$$u_{\mathrm{dc}} = q_{\mathrm{nq}} i_q \qquad (14)$$

The control effort of the dc voltage loop is deduced

$$i_{q1}^* = \frac{v_{\mathrm{dc}}}{-Z_{\mathrm{PF1}} i_q} u_{\mathrm{dc}}. \qquad (15)$$

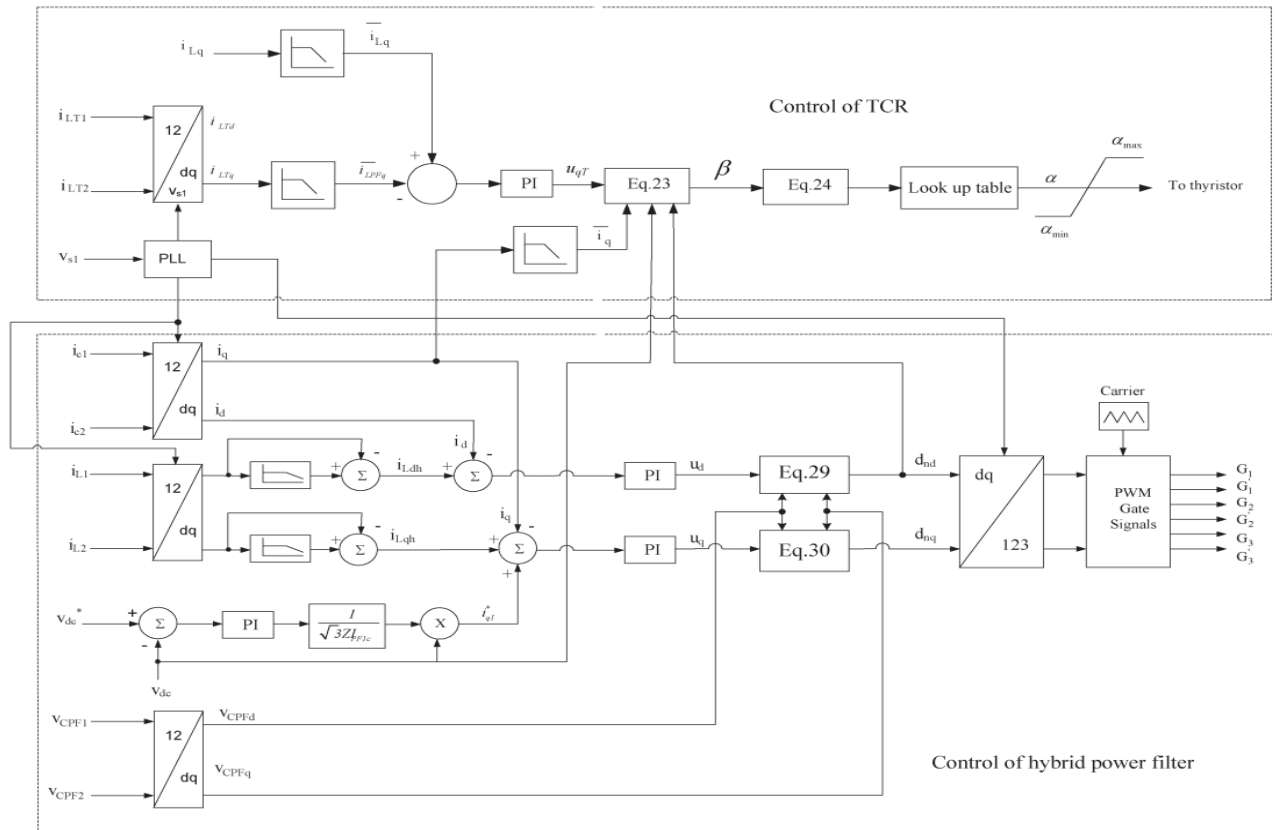The dc component will force the SHPF-TCR compensator to generate or to draw a current at the fundamental frequency.

Fig.3.Control scheme of the proposed SHPF-TCR compensator.

The response of the dc bus voltage loop is a second-order transfer function and has the following form:

$$\frac{V_{\mathrm{dc}}(s)}{V_{\mathrm{dc}}^*(s)} = 2\zeta\omega_{\mathrm{nv}} \frac{s + \frac{\omega_{\mathrm{nv}}}{2\zeta}}{s^2 + 2\zeta\omega_{\mathrm{nv}} s + \omega_{\mathrm{nv}}^2}$$

The closed-loop transfer function of dc bus voltage regulation is given as follows:

$$\frac{V_{\mathrm{dc}}(s)}{V_{\mathrm{dc}}^*(s)} = \frac{\frac{\sqrt{3}Z_{\mathrm{PF1}}k_p I_c}{\overline{V}_{\mathrm{dc}}C_{\mathrm{dc}}}s + \frac{\sqrt{3}Z_{\mathrm{PF1}}k_i I_c}{\overline{V}_{\mathrm{dc}}C_{\mathrm{dc}}}}{s^2 + \frac{\sqrt{3}Z_{\mathrm{PF1}}k_p I_c}{\overline{V}_{\mathrm{dc}}C_{\mathrm{dc}}}s + \frac{\sqrt{3}Z_{\mathrm{PF1}}k_i I_c}{\overline{V}_{\mathrm{dc}}C_{\mathrm{dc}}}}$$
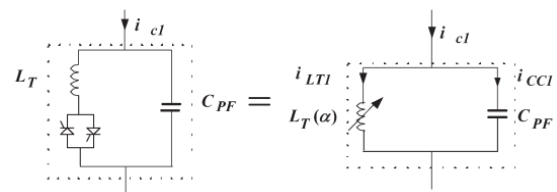

Fig.4.TCR equivalent circuit.

IV. MODELING OF TCR

Fig. 4 shows the TCR equivalent circuit. Using Kirchhoff's voltage law, the following equations in 123 reference frame are obtained:

$$v_{s1} = L_T \frac{di_{\mathrm{LT1}}}{dt} + L_{\mathrm{PF}} \frac{di_{c1}}{dt} + R_{\mathrm{PF}} i_{c1} + d_{n1} v_{\mathrm{dc}}$$

$$v_{s2} = L_T \frac{di_{\mathrm{LPF2}}}{dt} + L_{\mathrm{PF}} \frac{di_{c2}}{dt} + R_{\mathrm{PF}} i_{c2} + d_{n2} v_{\mathrm{dc}}$$

$$v_{s3} = L_T \frac{di_{LPF3}}{dt} + L_{PF}\frac{di_{c3}}{dt} + R_{PF}i_{c3} + d_{n3}v_{dc}$$
(19)

Applying Park's transformation, one obtains

$$L_T(\alpha)\frac{di_{LTd}}{dt} = L_T(\alpha)\omega i_{LTq} + L_{PF}\omega i_q - L_{PF}\frac{di_d}{dt} - R_{PF}i_d - d_{nd}v_{dc} + v_d$$

$$L_T(\alpha)\frac{di_{LTq}}{dt} = -L_T(\alpha)\omega i_{LTd} - L_{PF}\omega i_d - L_{PF}\frac{di_q}{dt} - R_{PF}i_q - d_{nq}v_{dc} + v_q.$$
(20)

The reactive part is chosen to control the reactive current   so

that $v_a = 0$ and $L_f(\alpha)\omega i_{LTd} = 0$

$$\frac{di_{LTq}}{dt} = B(\alpha)\omega\left[-L_{PF}\omega i_d - L_{PF}\frac{di_q}{dt} - R_{PF}i_q - d_{nq}v_{dc}\right]$$
(21)

whereB(α)=1/LF(α), $\omega$is the susceptance. An equivalent inputu$_{qT}$is defined as

$$u_{qT} = \frac{di_{LTq}}{dt}.$$
(22)

According to this expression, one deduces

$$B(\alpha) = \frac{u_{qT}}{\omega\left[-L_{PF}\omega i_d - L_{PF}\frac{di_q}{dt} - R_{PF}i_q - d_{nq}v_{dc}\right]}.$$
(23)

On the other hand, the equivalent inductance is given by

$$L_{PF}(\alpha) = L_{PF}\frac{\pi}{2\pi - 2\alpha + \sin(2\alpha)}.$$
(24)

The susceptance is given by

$$B(\alpha) = B\frac{2\pi - 2\alpha + \sin(2\alpha)}{\pi}$$
(25)

V.INDUCTION MOTOR

Induction Motor (1M) An induction motor is an example of asynchronous AC machine, which consists of a stator and a rotor. This motor is widely used because of its strong features and reasonable cost. A sinusoidal voltage is applied to the stator, in the induction motor, which results in an induced electromagnetic field. A current in the rotor is induced due to this field, which creates another field that tries to align with the stator field, causing the rotor to spin. A slip is created between these fields, when a load is applied to the motor.

Compared to the synchronous speed, the rotor speed decreases, at higher slip values. The frequency of the stator voltage controls the synchronous speed [12]. The frequency of the voltage is applied to the stator through power electronic devices, which allows the control of the speed of the motor. The research is using techniques, which implement a constant voltage to frequency ratio. Finally, the torque begins to fall when the motor reaches the synchronous speed. Thus, induction motor synchronous speed is defined by following equation,

$$n_s = \frac{120f}{p}$$

Where f is the frequency of AC supply, n, is the speed of rotor; p is the number of poles per phase of the motor. By varying the frequency of control circuit through AC supply, the rotor speed will change.

VI.MATLAB/SIMULINK RESULTS

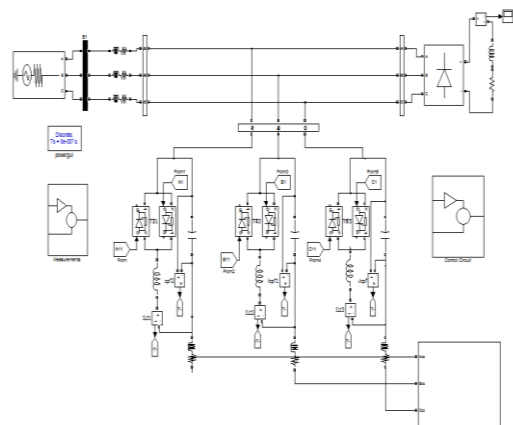*Case 1: Performance of SHPF-TCR for harmonic generated load*

Fig.5.Simulink circuit for SHPF-TCR under harmonic generated load

International Journal of Research

Available at https://edupediapublications.org/journals

e-ISSN: 2348-6848
p-ISSN: 2348-795X
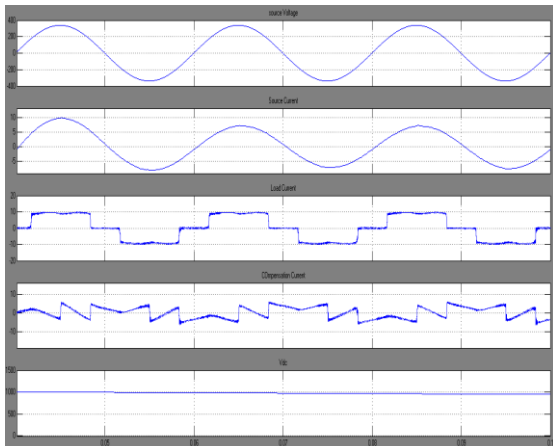Volume 04 Issue-17
December 2017

Fig.6.Simulation results for source voltage, source current, load current, compensation currents and dc link voltage
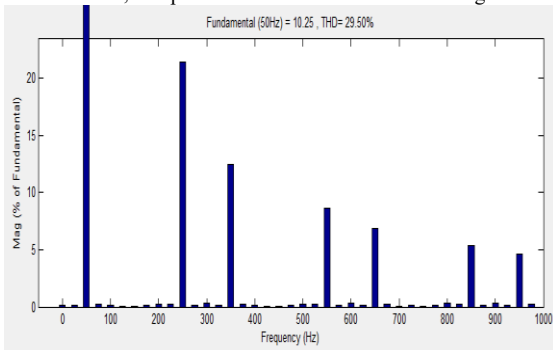

Fig.7.Harmonic spectrum for source current without compensation
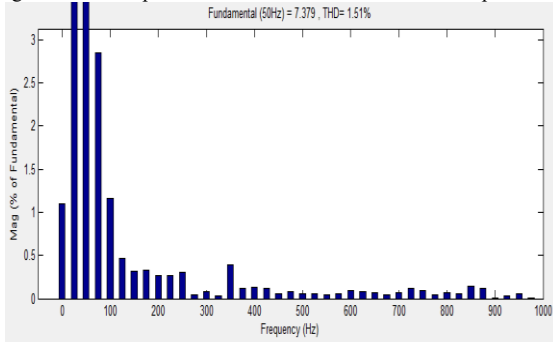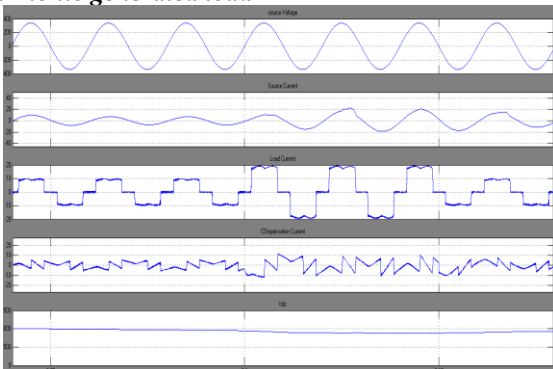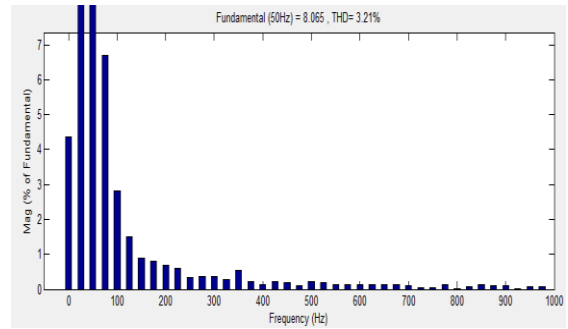

Fig.8.Harmonic spectrum for source current with compensation

Case 2: Performance of SHPF-TCR for distorted harmonic generated load

Fig.9.Simulation results for source voltage, source current, load current, compensation currents and dc link voltage.

Fig.10.Harmonic spectrum for source current with compensation

Case 3: Performance of SHPF-TCR for harmonic and reactive type load
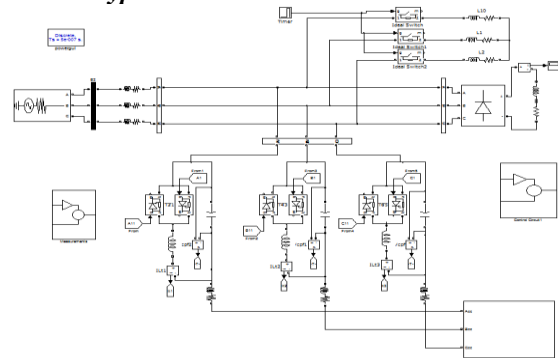

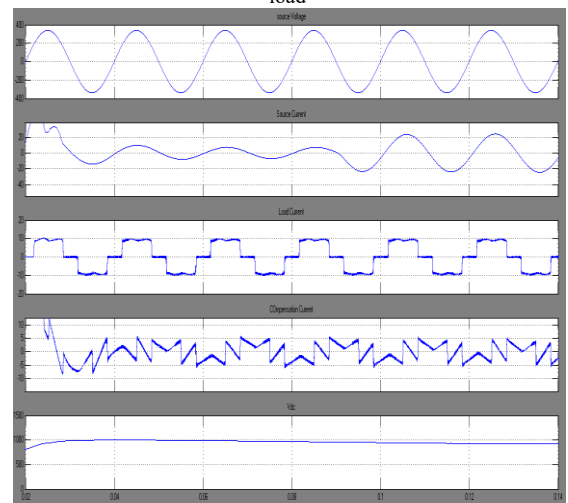Fig.11.Simulink circuit for SHPF-TCR for harmonic and reactive type load

Fig.12.Simulation results for source voltage, source current, load current, compensation currents and dc link voltage
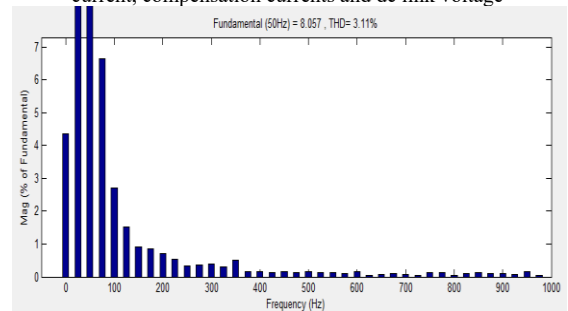

Fig.13.Harmonic spectrum for source current with compensation

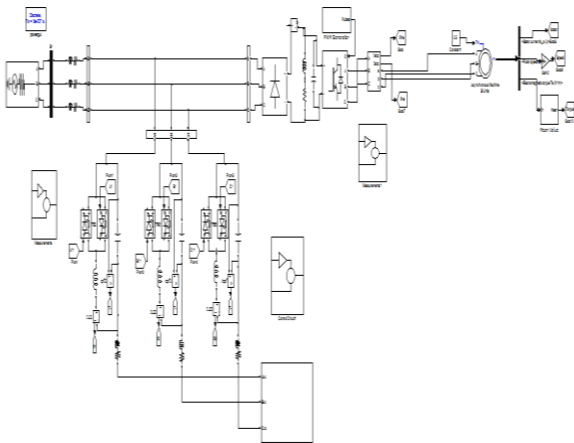*Case 4: Performance of SHPF-TCR for harmonic generated load with induction motor*

Fig.14.Simulink circuit for SHPF-TCR for harmonic and reactive type load with induction motor
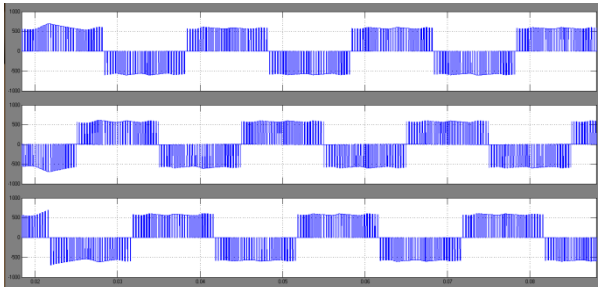

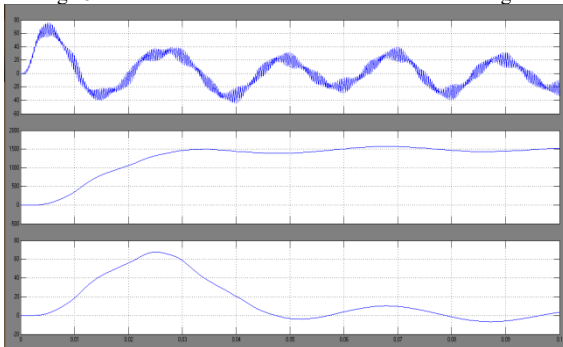Fig.15.Simulation results for inverter line to line voltages

Fig.16.Simulation results for Current,speed and torque

VII. CONCLUSION

In this paper, a SHPF-TCR compensator of a TCR and a SHPF has been proposed to achieve harmonicelimination and reactive power compensation. A proposed nonlinear control scheme of a SHPF-TCRcompensator has been established and simulated. The shunt active filter and SPF have a complementary function to improve the performanceof filtering and to reduce the power rating requirements of an active filter. The scheme has the advantage ofsimplicity and is able to provide self-supported dc bus of the active filter through power transfer from ac line atfundamental frequency. Power quality improvement for proposed system we can reduce the source current harmonics and fed with three phase inverter for the application of induction motor performance of speed torque characteristics.

REFERENCES

[1] A. Hamadi, S. Rahmani, and K. Al-Haddad, "A hybrid passive filter configuration for VAR control and harmonic compensation," IEEE Trans. Ind. Electron., vol. 57, no. 7, pp. 2419–2434, Jul. 2010.

[2] P. Flores, J. Dixon, M. Ortuzar, R. Carmi, P. Barriuso, and L. Moran, "Static Var compensator and active power filter with power injection capability, using 27-level inverters and photovoltaic cells," IEEE Trans.Ind. Electron., vol. 56, no. 1, pp. 130–138, Jan. 2009.

[3] X. Wang, F. Zhuo, J. Li, L. Wang, and S. Ni, "Modeling and control of dual-stage high-power multifunctional PV system in d-q-0 coordinate," IEEE Trans. Ind. Electron., vol. 60, no. 4, pp. 1556–1570, Apr. 2013.

[4] J. A. Munoz, J. R. Espinoza, C. R. Baier, L. A. Moran, E. E. Espinosa, P. E. Melin, and D. G. Sbarbaro, "Design of a discrete-time linear control strategy for a multicell UPQC," IEEE Trans. Ind. Electron., vol. 59, no. 10, pp. 3797–3807, Oct. 2012.

[5] L. Junyi, P. Zanchetta, M. Degano, and E. Lavopa, "Control design and implementation for high performance shunt active filters in aircraft power grids," IEEE Trans. Ind. Electron., vol. 59, no. 9, pp. 3604–3613, Sep. 2012.

[6] Z. Chen, Y. Luo, and M. Chen, "Control and performance of a cascaded shunt active power filter for aircraft electric power system," IEEE Trans. Ind. Electron., vol. 59, no. 9, pp. 3614–3623, Sep. 2012.

[7] S. Rahmani, A. Hamadi, K. Al-Haddad, and A. I. Alolah, "A DSP-based implementation of an instantaneous current control for a three-phase shunt hybrid power filter," J. Math. Comput. Simul.—Model. Simul. Elect. Mach., Convert. Syst., vol. 91, pp. 229–248, May 2013.

[8] A. Hamadi, S. Rahmani, and K. Al-Haddad, "Digital control of hybrid power filter adopting nonlinear control approach," IEEE Trans. Ind. Informat., to be published.

[9] A. Bhattacharya, C. Chakraborty, and S. Bhattacharya, "Parallelconnected shunt hybrid active power filters operating at different switching frequencies for improved performance," IEEE Trans. Ind. Electron., vol. 59, no. 11, pp. 4007–4019, Nov. 2012.

[10] S. Rahmani, A. Hamadi, N. Mendalek, and K. Al-Haddad, "A new control technique for three-phase shunt hybrid power filter," IEEE Trans. Ind. Electron., vol. 56, no. 8, pp. 2904–2915, Aug. 2009.

[11] A. Luo, X. Xu, L. Fang, H. Fang, J. Wu, and C. Wu, "Feedbackfeedforward PI-type iterative learning control strategy for hybrid active power filter with injection circuit," IEEE Trans. Ind. Electron., vol. 57, no. 11, pp. 3767–3779, Nov. 2010.

[12] M. I. Milanés-Montero, E. Romero-Cadaval, and F. Barrero-González, "Hybrid multi-converter conditioner topology for high-power applications," IEEE Trans. Ind. Electron., vol. 58, no. 6, pp. 2283–2292, Jun. 2011.

[13] A. Luo, S. Peng, C. Wu, J. Wu, and Z. Shuai, "Power electronic hybrid system for load balancing compensation and frequency-selective harmonic suppression," IEEE Trans. Ind. Electron., vol. 59, no. 2, pp. 723– 732, Feb. 2012.

[14] A. Luo, Z. Shuai, W. Zhu, and Z. John Shen, "Combined system for harmonic suppression and reactive power compensation," IEEE Trans. Ind. Electron., vol. 56, no. 2, pp. 418–428, Feb. 2009.